

# Mnemosyne: Parallelization Strategies for Efficiently Serving Multi-Million Context Length LLM Inference Requests Without Approximations

Amey Agrawal<sup>2</sup>, Junda Chen<sup>3</sup>, Íñigo Goiri<sup>1</sup>,  
Ramachandran Ramjee<sup>1</sup>, Chaojie Zhang<sup>1</sup>, Alexey Tumanov<sup>2</sup>, and Esha Choukse<sup>1</sup>

<sup>1</sup>Microsoft

<sup>2</sup>Georgia Institute of Technology

<sup>3</sup>UC San Diego

## Abstract




As large language models (LLMs) evolve to handle increasingly longer contexts, serving inference requests for context lengths in the range of millions of tokens presents unique challenges. While existing techniques are effective for training, they fail to address the unique challenges of inference, such as varying prefill and decode phases and their associated latency constraints – like Time to First Token (TTFT) and Time Between Tokens (TBT). Furthermore, there are no long context inference solutions that allow batching requests to increase the hardware utilization today.

In this paper, we propose three key innovations for efficient interactive long context LLM inference, without resorting to any approximation: adaptive chunking to reduce prefill overheads in mixed batching, Sequence Pipeline Parallelism (SPP) to lower TTFT, and KV Cache Parallelism (KVP) to minimize TBT. These contributions are combined into a 3D parallelism strategy, enabling Mnemosyne to scale interactive inference to context lengths at least up to 10 million tokens with high throughput enabled with batching. To our knowledge, Mnemosyne is the first to be able to achieve support for 10 million long context inference efficiently, while satisfying production-grade SLOs on TBT (30ms) on contexts up to and including 10 million.

## 1 Introduction

Emerging applications are pushing large language models (LLMs) to process contexts orders of magnitude longer than current systems support. Tasks like book summarization, movie analysis, multi-agent dialogues with extensive knowledge retrieval, and multi-modal reasoning demand models capable of retaining and reasoning over millions of tokens (Figure 1).

Correspondence to: Amey Agrawal <ameyagrawal@gatech.edu>, Esha Choukse <esha.choukse@microsoft.com>.

	Prefill Latency	Decode Latency
<b>1M Tokens</b> 5 Books 700K Words 	14 Secs	64 Tokens/s
<b>5M Tokens</b> 4 Audiobooks 55 Hours 	3.5 Mins	56 Tokens/s
<b>10M Tokens</b> 4 Movies 10 Hours 	10.6 Mins	40 Tokens/s

**Figure 1:** Mnemosyne’s performance on extreme-length contexts. The system can support up requests with up to 10 million tokens with low latencies by efficiently scaling across 128 NVIDIA H100 GPUs, maintaining interactive speeds even for massive inputs.

Recently, *ring and striped attention* mechanisms [11, 30] have emerged as powerful tools for training LLMs with long contexts. However, these techniques do not extend well to inference, where the dynamics differ significantly due to the complexities of differences in prefill and decode phases with the distinct latency metrics: Time to First Token (TTFT) and Time Between Tokens (TBT). Inference services also require handling mixed workloads with varying context lengths, and ring/striped attention falls short in such scenarios because of rigid parallelism and head-of-line (HOL) blocking, a situation where small requests are inordinately delayed behind large prefill operations. This paper addresses these gaps by introducing Mnemosyne, a system that provides scalable and efficient long-context inference solutions.

The first challenge Mnemosyne tackles is HOL blocking. A naive solution is to chunk the input into smaller pieces as suggested by previous work [7, 19]. However, chunking introduces read amplification (i.e., large quadratic overheads in GPU memory reads), leading to the prevailing wisdom that the chunking overhead will increase significantly with increase in context lengths [51]. Surprisingly, we show the opposite to be true, i.e., the chunking overhead due to quadratic

read amplification is high for small prefills, but this overhead reduces as context length increases! In fact, even an extremely small chunk of size 32 incurs only a marginal overhead for attention prefill computation as shown in Figure 7. Thus, chunking of long context prefills is a key mechanism that helps circumvent HOL blocking. However, choosing the right chunk size presents a continuous trade-off between chunking overhead and maintaining the latency targets for the ongoing prefill and decode phases. Thus, Mnemosyne proposes **adaptive chunking**, a dynamic approach to chunk sizing based on workload characteristics.

The second challenge lies in minimizing TTFT. Traditional parallelism strategy for this, *tensor parallelism* (TP), is insufficient to meet the latency requirements, as it cannot scale beyond a single server due to the slower interconnects between GPUs across different servers. To address this, we combine another traditional solution, *pipeline parallelism* (PP) with adaptive chunking and a more efficient pipeline use during prefill, thereby processing the prefill chunks of a long request in parallel. We refer to this approach as **sequence pipeline parallelism** (SPP) and this enables significant reductions in TTFT.

The third major challenge is TBT, where neither TP, PP, nor SPP offer adequate improvements for very large context requests. To address this, Mnemosyne introduces **KV Cache Parallelism (KVP)**, which distributes the key-value cache across multiple workers across servers during the decode phase, effectively parallelizing and accelerating token generation.

With Mnemosyne, we propose an innovative combination of TP, adaptive chunking with SPP, and KVP, resulting in a new 3D parallelism implementation. Mnemosyne enables exact inference with long contexts, while achieving performance scaling for context lengths at least up to 10 million tokens — a first in the field!

In summary, we make the following contributions to long context inference, without adding any approximation:

- **Sequence pipeline parallelism (SPP)**, a novel strategy combining prefill chunking and pipeline parallelism to deal with head-of-line blocking during multi-million context prefill without compromising on the TTFT latency.
- **Adaptive chunking** and **KV cache parallelism (KVP)** to dynamically trade-off the TTFT and TBT across requests batched together.
- **Mnemosyne 3D parallelism**, combining TP, SPP, and KVP. We demonstrate the first system to scale LLM inference at least up to 10 million tokens, meeting stringent latency requirements while maintaining efficiency through mixed batching across various context lengths.

<i>Parallelism Strategy</i>	Batchable	Preemptable*	Faster Prefills	Faster Decodes	Scalability
Pipeline Parallelism (PP) [21]	✓	✓	×	×	↑
Tensor Parallelism (TP) [42]	✓	✓	✓	✓	↓
Ring/Striped Attention (RA) [11, 30]	×	×	✓	×	↑
Sequence Pipeline Parallelism (SPP)	✓	✓	✓	×	↑
KV Parallelism (KVP)	✓	✓	✓	✓	↓
<b>Mnemosyne 3D Parallelism (3DP)</b>	✓	✓	✓	✓	↑

**Table 1:** Comparison of Parallelization Techniques for Long Context LLM Inference. \*Preemptability shows whether the parallelism strategy can be combined with chunked prefills for fine-grained pre-emption support.

## 2 Background and Motivation

### 2.1 Long Context Transformers

Auto-regressive generative transformer models operate in two phases during inference. The prefill phase processes the input context, building internal representations of all input tokens (KV cache). The subsequent decode phase generates output tokens one by one, based on previously processed context.

Recent research has demonstrated that large language models can be fine-tuned to handle context lengths spanning millions of tokens. This is achieved by re-scaling positional embeddings [10, 29, 46]. These long-context transformers unlock new capabilities, including multi-modal processing and reasoning over several books’ worth of textual data. Google’s Gemini 1.5 model [39] exemplifies these advancements, with support for up to 2 million context length in production.

However, this expanded context window introduces significant computational challenges, particularly in the prefill phase where complexity grows quadratically with input size. The tension between these expanded capabilities and the associated computational demands form the core challenge addressed in this work.

To illustrate the magnitude of challenges in serving LLMs with long context lengths, let’s consider Llama-3 70B as an example. For a long request with a million tokens, we need 320 GB for memory to just store the KV cache, and a massive 2.4 exaFLOPs for prefill computation.

### 2.2 Performance Metrics

The inference performance of transformer models is characterized by three key metrics:

**Time to First Token (TTFT):** The latency from input submission to first output token generation. TTFT is determined by the prefill phase and is critical for interactive applications.

**Time Between Tokens (TBT):** The delay between consec-

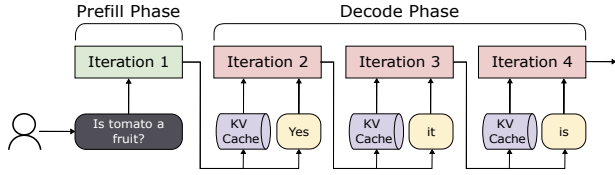


**Figure 2:** The two phase inference process in generative transformer models. First, the input prompt is processed in the prefill phase, subsequently, output tokens are generated sequentially during the decode phase using the KV cache.

utive token generations during the decode phase. TBT affects the perceived fluency of model output.

**Throughput:** The request load that an online inference serving system can sustain while satisfying Service Level Objective (SLO) constraints on request latency. Throughput captures the overall system efficiency.

These metrics capture the fundamental tension between latency and efficiency in serving systems. Optimizing for one often involves trade-offs with the other, necessitating careful system design to balance performance across different use cases.

**Long Context Inference.** Current production services [22, 39] support interactive inference for requests up to one million tokens, achieving TTFT of  $\sim 50$  seconds and TBT of  $\sim 20$ ms. However, as context length approaches 10 million tokens, the quadratic complexity of attention operations makes interactive prefill increasingly challenging. To address this, operators have introduced on-demand context caching [44, 45]. This functionality allows users to ingest long prompts as batch jobs, then leverage the resulting KV cache for interactive processing of the followup queries.

### 2.3 Popular Parallelism Strategies

Modern large transformer models – with billions of parameters and complex architectures – necessitate distributed computation across multiple processors to achieve high throughput with interactive latencies.

**Pipeline Parallelism (PP)** splits the model layers across different stages, each running on a separate device. As one stage finishes processing a batch of data, it passes it to the next stage. By splitting the memory load across multiple devices, pipeline parallelism frees up more memory for KV cache, thereby enabling higher batch sizes and throughput. The communication between two stages is minimal in PP, allowing to scale inference across several nodes. However, a key limitation of pipeline parallelism is that it does not help with improving inference latency due to sequential dependency between pipeline stages.

On the other hand, **Tensor Parallelism (TP)** divides tensors within individual model layers, distributing matrix operations (e.g., those in attention mechanisms) across multiple

devices (Figure 3). By parallelizing computation at intra-layer granularity, TP enables faster execution of large operations and reduces memory bottlenecks. Consequently, tensor parallelism is effective at both improving latency and throughput of the system.

However, frequent and large communication operations in tensor parallelism require low latency and high bandwidth. This constrains TP’s scalability to the NVLINK domain (typically within a single compute node on current hardware), in contrast to PP’s broader scalability. In practice, PP and TP are often combined to optimize resource utilization, minimize latency, and maximize throughput.

**Long Context Inference.** While a combination of PP and TP enables scaling out inference deployment to meet the memory requirements of long context inference, only TP contributes to latency reduction. However, TP’s scaling is constrained to a single node. Consequently, when serving requests with millions of tokens, these traditional parallelization approaches fall short in achieving latency objectives.

### 2.4 Batching Policies

In inference systems, one of the most common ways to increase utilization and throughput is to batch execution of multiple requests together. Orca [49] introduced continuous batching wherein requests can dynamically enter or exit a batch at the granularity of individual iterations. However, naively performing iteration-level batching can result in high-tail decode latency due to interference from long prefill requests [7]. In order to concurrently achieve high-throughput and low-latency, two popular strategies have emerged the address this prefill-decode interference challenge:

**Chunked Prefills** [7, 8, 19] is a technique to divide the input context into smaller chunks and piggyback the prefill computation of these chunks with existing decode iterations. This mixed batching approach allows efficient computation of prefills at a small delta cost, with predictable decode latency.

Figure 4 shows the scheduling of prefill chunks of request B in this approach, unblocking decode phases of request A.

**Prefill-Decode Disaggregation** [35, 51] on the other hand, decouples the execution of prefill and decode phases and splits their computation onto different devices. The dedicated prefill and decode devices run homogeneous batches, with much more predictable latency.

**Long context inference.** Although chunked prefill is effective at reducing decode latency, previous studies [8, 51] suggest that prefill computation with chunking becomes inefficient due to KV cache read amplification, deeming the mechanism unsuitable for long-context inference. On the other hand, the disaggregation techniques require moving the whole KV cache between the prefill and decode devices. This reduces the memory available for the KV cache, making disaggregation less appealing for long context inference where the KV cache can span hundreds of GBs.

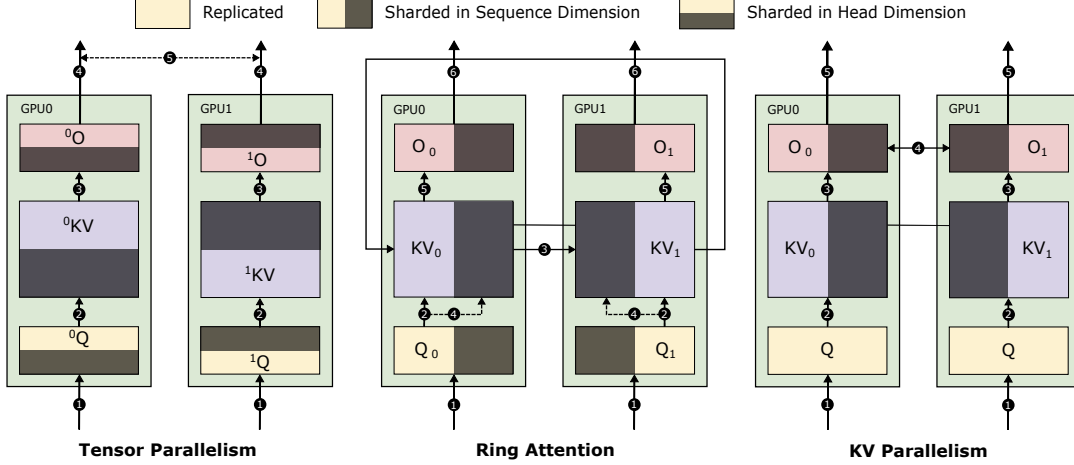


**Figure 3:** Comparison of parallelization strategies for transformer attention. Tensor Parallelism (TP) shards computation across the head dimension, Ring Attention (RA) distributes computation across the sequence dimension with cyclic KV cache transfers, and KV Parallelism (KVP) shards the KV cache across GPUs. Arrows indicate data flow, with numbered steps showing the computation order.

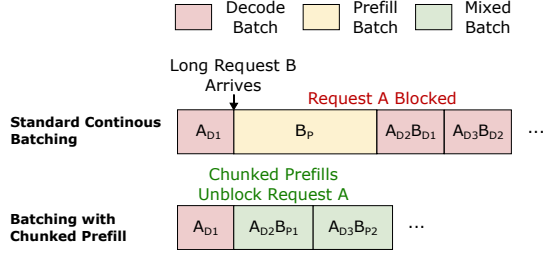


**Figure 4:** Impact of chunked prefills on continuous batching. Standard continuous batching (top) shows head-of-line blocking when a long request B arrives, delaying subsequent decodes of request A. Chunked prefill batching (bottom) piggybacks prefill chunks of B with decodes of A, reducing latency for both requests and improving overall throughput.

Notation	Definition
$n$	number of tokens
$n_q$ or $n_{kv}$	number of query or key-value tokens
$l$	number of layers
$h_q$ or $h_{kv}$	number of query or key-value heads
$d$	attention head dimension
$p$	total number of workers
$p_j$	parallelism degree for strategy $j$ . e.g. $p_{1p}$ for TP
$M_{kv}$	memory required for KV cache
$F_a$	attention flops
$R_a$	number of bytes read for attention
$I_a$	attention arithmetic intensity
$c$	chunk size
$T$	execution time
$T_p$ or $T_d$	prefill latency or decode latency

**Table 2:** Definitions of notations in equations.

### 3 Challenges

Serving extremely long context requests strains computational resources, challenges system efficiency, and pushes the boundaries of achievable latency. In this section, we explore the fundamental technical challenges that make supporting long context inference challenging.

#### 3.1 Resource Demands

The two primary phases of LLM inference – prefill and decode – exhibit distinct resource requirements [8, 35]. The prefill phase is compute intensive, due to the concurrent processing of several prompt tokens in a batched manner. In contrast, the decode phase is memory bound due to sequential generation of each decode token.

As the context length of requests increases, the resource requirement across each of these phases grows asymmetrically.

We analyze the resource requirements across three primary axis – computational FLOPs, memory bandwidth, and memory capacity. Table 2 shows the notation used across the paper.

During the prefill process, each prompt token needs to attend to all the prior tokens in the sequence. As a result, the arithmetic operations required for prefill attention computation grow quadratically. For a prompt with  $n$  input tokens, the computational FLOPs ( $F_a(n)$ ) can be captured as follows:

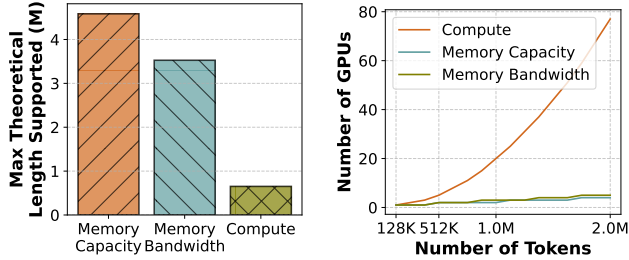
$$F_a(n) = 4n^2dh_q \quad (1)$$

Subsequently, during the decode phase, we need to scan through the entire prompt KV cache, which results in linear increase in memory reads. Memory capacity requirement for the KV cache ( $M_{kv}(n)$ ), and memory reads ( $R_a(n)$ ) for decode phase can be computed as:

$$M_{kv}(n) = 4ndh_{kv} \quad (2)$$

$$R_a(n) = M_{kv}(n) = 4ndh_{kv} \quad (3)$$





(a) Maximum number of tokens supported per resource type on 8 H100 GPUs. (b) Number of GPUs required to meet each resource needed for given context length.

**Figure 5:** Theoretical resource requirements for serving Llama-3 8B with 30s TTFT and 20ms TBT SLOs, illustrating compute as the primary scaling bottleneck for interactive long-context LLM inference workloads.

Note that while the prefill computational FLOPs increases quadratically with the number of input tokens, the KV cache memory requirement only grows linearly.

There are existing online inference services like Gemini [39], that serve inference for 1M input context with a sub-one minute time to first token and over forty tokens per second output rate. Figure 5a shows the theoretical maximum number of input tokens that can meet the SLO of 30s TTFT and 20ms TBT on a single DGX-H100 node for Llama-3 8B. Compute quickly becomes a bottleneck at 768K input tokens, while memory capacity scales the most.

Conversely, Figure 5b shows the number of GPUs needed to meet this TTFT and TBT SLO as the number of input tokens increase. 20 GPUs are needed for 1M context length, and 80 GPUs for 2M input context. Production serving systems like Gemini aim to provide interactive user interface that could enable processing and analysis of large input prompts – as a result, the SLO for prefill processing cannot grow quadratically with the prompt length even if the compute requirements do. This dichotomy leads to a stark skew in the resource requirements where the quadratic compute in prefill phase become the most significant bottleneck.

### 3.2 Parallelizing Long Context Computation

Recent works [11, 30] have proposed new attention parallelism techniques to tackle the computational needs for training of long context transformer models. **Ring Attention** [30], as shown in Figure 3, proposes to parallelize computation across the sequence dimension by partitioning the query across participating workers. Each worker is responsible for the computation of a shard of query tokens. At the beginning, each worker performs attention computation with the query (Q) and key-value (KV) blocks from the shard assigned to it. Subsequently, each worker transfers its KV block to the next worker, while concurrently receiving the KV block from the

previous worker in a ring formation. This allows each query shard to attend to all the KV shards. For better efficiency, Liu et al. [30] overlap the attention computation of each block with the KV cache transfer.

The causal nature of attention in modern LLMs (where each token only needs to attend to tokens prior to itself), leads to a workload imbalance in Ring Attention – where each worker is assigned a query block sequentially without accounting for the causal masking. **Striped Attention** [11] addresses this challenge by assigning non-contiguous strips of query tokens to each worker such that workload across all the workers is divided almost uniformly resulting in upwards of  $1.5\times$  speedup compared to Ring Attention.

However, adopting these state-of-the-art training parallelization techniques for inference presents several challenges:

**C1. Head-of-line blocking:** Ring and striped attention do not allow preemption of a long context prefill phase. For multi-million context lengths, this can cause head-of-line blocking that can last several minutes.

**C2. Batching support:** Ring and striped attention as applied to inference can help solely with reducing prefill latency. These parallelization approaches do not support batching, or mixed batching. This leads to low system utilization and throughput.

**C3. Rigid parallelism and variable input lengths:** In a real world service, the input sequences are of various lengths [35], ranging from 10s to 1000s, and now millions of tokens. The way ring and striped attention distribute tokens across GPUs is optimized for the longest context they need to serve within a latency SLO. However, this distribution is rigid, and has to be reused for smaller requests. Building upon Equations (1) and (3), the following equation shows the arithmetic intensity of attention:

$$I_a(n) \simeq \frac{F_a(n)}{R_a(n)} = n \frac{h_q}{h_{kv}} \quad (4)$$

Thus, the arithmetic intensity of attention prefill operation is directly proportional to the number of tokens. In ring attention, the  $n$  input tokens are distributed evenly across all the participating workers ( $p_{ra}$ ), resulting in proportionate decrease in the arithmetic intensity of the operation. Consequently, when the number of tokens per worker becomes too small, the operation becomes memory/network bound and the KV cache block transfers become the bottleneck. Thus the optimal parallelization degree in ring attention is dependent on the sequence length.

This create a trade-off between latency objectives and hardware utilization. If the deployment is optimized for minimizing latency of long context requests (with large number of workers), the hardware utilization suffers for shorter requests and vice versa.

**C4. Lacking support for decode computation:** Since ring and striped attention were both originally proposed for long context training, they can be used to parallelize the prefill

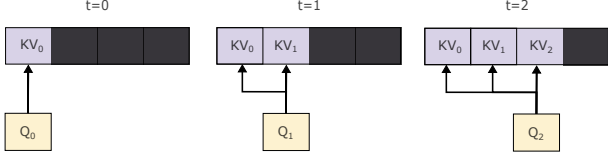


**Figure 6:** Illustration of KV cache read amplification in chunked prefill over time. As new chunks ( $Q_1$ ,  $Q_2$ ) are processed, they must again read all previously computed KV cache, leading to quadratic growth in total reads. This phenomenon was previously thought to make chunked prefills inefficient for long contexts.

phase of the long context inference, but do not directly extend to the decode phase. This renders these solutions incomplete for long context inference, and calls for a solution for the end-to-end long context inference.

### 3.3 Requirements from an Efficient Long Context Serving System

As shown above, existing techniques like ring/striped attention [11, 30] do not meet the needs of long context LLM inference. Based on our analysis, to build an efficient long context serving system, we need to:

- R1:** Meet the stringent TTFT and TBT SLOs of long context interactive services.
- R2:** Drive up the hardware utilization to increase throughput per device, and reduce the cost per inference.
- R3:** Efficiently handle a wide range of context length requests at the same time within a single system.

## 4 Mnemosyne: System Design

### 4.1 Revisiting Chunked Prefills for Long Context

As described in Section 2.4, distributing the input prompt into smaller chunks for prefill phase allows better scheduling across requests and prefill/decode phases. This is because the maximum batch processing time can now be decoupled from the input length of the prefill request.

This technique holds a lot of promise for supporting batching in long context LLM inference. However, previous analyses [8, 51] concluded that chunked prefills were unsuitable for long context handling due to read amplification.

The following equation shows the amount of data read into the GPU cores during a contiguous prefill phase for a request with  $n$  input tokens:

$$R_a(n) = M_{kv}(n) = 4ndh_{kv} \quad (5)$$

Since the chunked prefill technique temporally distributes a single prefill phase across several forward passes of the model, the total reads increase linearly with number of chunks. This

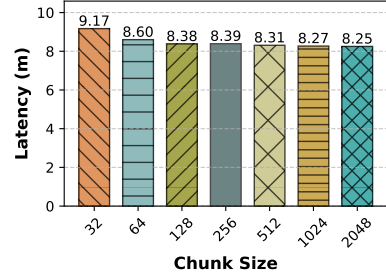


**Figure 7:** Impact of chunk size on attention computation time for a 1M tokens prefill with Llama-3 70B using 8 H100s. Even very small chunk sizes (32-128 tokens) only incur marginal overhead compared to larger chunk sizes. This demonstrates that attention computation remains efficient with small chunks, contradicting previous assumptions about chunked prefills for long contexts.

is depicted in Figure 6. Different parts of the query  $Q$  are scheduled sequentially. However, each  $Q_n$  needs to attend to the KV cache from all the previous chunks. This read amplification can be formulated as follows:

$$R_{cp}(n, c) = \sum_{i=1}^{n/c} R_a(ic) = O(n^2) \quad (6)$$

This read amplification from chunked prefill increases the cache reads from  $O(n)$  to  $O(n^2)$ . Leading to the belief that chunked prefills for inefficient at processing long context requests. We challenge this view by examining the problem through the lens of arithmetic intensity.

Our key insight is that the arithmetic intensity of a prefill chunk depends solely on the chunk size, not the sequence length. This counter-intuitive result arises because in chunked prefills, even though processing of each chunk requires us to fetch all the previously generated KV-cache tokens from memory, we also need to perform  $c$  arithmetic operations for each of the KV-cache token – corresponding to each token in the prefill chunk. Thus, while longer sequences do require more KV-cache reads, the number of arithmetic operations per read remains constant, determined by the chunk size.

Modern LLMs further amplify this effect through grouped-query attention [9] as shown in Equation (7). In Llama-3 70B, for instance, 8 query heads share a single KV head, boosting arithmetic intensity approximately 8-fold compared to linear layers [7]. This leads to a surprising conclusion: on NVIDIA H100 GPUs, **a prefill chunk of merely ~40 tokens suffices to saturate GPU compute**. This observation enables us to implement effective batching and fine-grained preemption policies by decomposing multi-million token prefills into thousands of small, manageable chunks. Each chunk executes in tens of milliseconds, contrasting sharply with ring-attention’s minutes-long, monolithic prefill computations.

$$I_{cp}^i(n, c) = \frac{F_{cp}^i(n, c)}{R_{cp}^i(n, c)} \simeq \frac{4ic^2dh_q}{4icdh_{kv}} = c \frac{h_q}{h_{kv}} \quad (7)$$

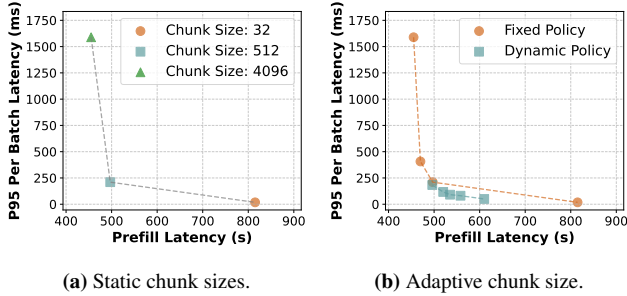


**Figure 8:** Pareto frontiers demonstrating superior performance of adaptive chunking for balancing prefill and decode latencies in mixed batching. (a) Static chunk sizes force a trade-off: larger chunks reduce prefill latency but increase per-batch (decode) latency. (b) Adaptive chunk sizing policy starts with larger chunks and progressively reduces the chunk size such the latency of each batch remains similar. This allows for a better compromise between prefill efficiency and maintaining low decode latency for mixed workloads.

We have identified an additional factor that led to the mis-characterization of chunked prefills for longer contexts in prior studies [8]. Traditional attention kernels parallelized prefill computation by distributing work across query tokens. This approach is effective for standard prefill operations where query and KV token counts are equal. However, it falls short in chunked prefills, where the limited number of query tokens constrains parallelization opportunities.

Recently, FlashDecoding [20] introduced a method to accelerate decode computations for long requests by sharding work across KV tokens. Building on this insight, state-of-the-art attention kernels [14, 48] now parallelize prefill computation across both query and KV token dimensions. This two-dimensional parallelization strategy enables efficient chunked prefill computation, even for very long contexts.

## 4.2 Adaptive Chunked Prefills

Figure 7 shows that using a chunk size of 32 leads to only a moderate overhead of 11% compared to chunk size of 2048 in attention computation. However, operating with a small chunk size can result in significant end-to-end performance degradation due to inefficient computation of linear layers and other fixed CPU overheads. For Llama-3 8B running on 8 NVIDIA H100 GPUs, we observe that chunk size of 32 has 1.75 $\times$  higher prefill latency for a 1 million token request compared to the chunk size of 4096. On the other hand, larger chunk sizes lead to higher decode latency for requests that are batched along as shown in Figure 8a. This leads to an undesirable trade-off between prefill and decode latency.

To avoid this trade-off we adopt a dynamic chunk size adjustment policy. This policy is based on the observation that the later iterations of prefill processing where the per chunk latency is high, the fraction of attention runtime dominates over other overheads – as a result, smaller chunks become more ef-

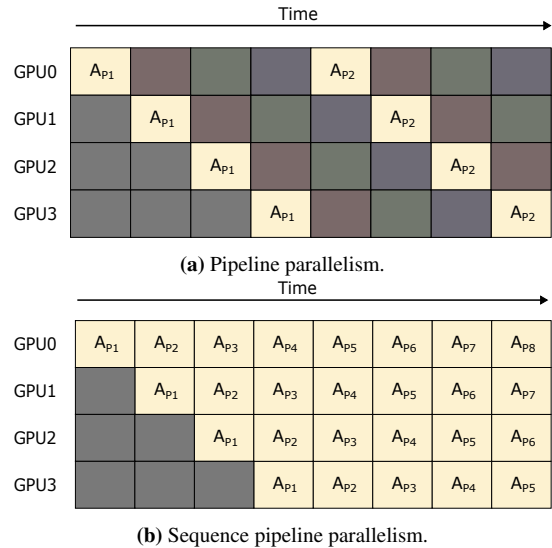


**Figure 9:** Contrasting pipeline parallelism strategies for prefill processing. (a) Standard pipeline parallelism uses micro-batches to improve throughput, but doesn’t reduce latency for long sequences. (b) Sequence pipeline parallelism (SPP) overlaps chunk processing across stages, significantly reducing prefill latency for long contexts while maintaining high GPU utilization.

ficient in the later phase of prefill processing. To maintaining low decode latency without sacrificing prefill efficiency, we start with a large chunk size and dynamically reduce it as we progress in the prefill. We adopt runtime prediction component from the Vidur simulator [6] to identify the largest chunk size that can be used processed without violating decode latency SLO. Adaptive chunking allows to obtain significantly better prefill-decode latency trade-off as shown in Figure 8b.

This approach lays the groundwork for future extensions that could incorporate more complex scheduling objectives, such as fairness [40] or deadline-aware scheduling [5].

## 4.3 Sequence Pipeline Parallelism

The quadratic increase in prefill latency with sequence length poses a significant challenge for user experience. While tensor parallelism has traditionally been used to reduce latency, it faces scaling limitations beyond a single compute node due to high communication overhead. Pipeline parallelism, though efficient in scaling across multiple GPUs, primarily improves throughput rather than latency.

We introduce a critical insight – combining chunked prefills with pipeline parallelism can substantially reduce prefill latency through an optimized pipelining schedule. Conventional PP inference systems [7, 49] use interleaved micro-batches to maintain pipeline efficiency. For a request  $A$ , chunk  $i + 1$  is typically scheduled only after chunk  $i$  completes all pipeline stages (Figure 9a). While necessary for auto-regressive decoding, this approach is sub-optimal for the prefill phase, where

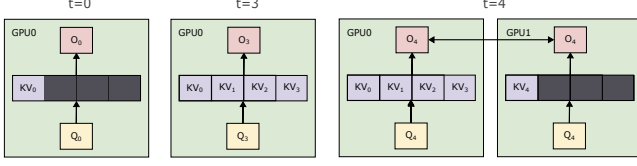


**Figure 10:** KV Parallelism (KVP) dynamically scales resources as the processed context length grows. Initially, a single GPU stores the KV cache ( $t=0$ ). As more chunks are processed, the cache expands within the GPU ( $t=3$ ). When a single GPU’s latency capacity is reached, KVP adds a new GPU ( $t=4$ ) to accommodate further growth. This progressive scaling enables KVP to bound per chunk latency even for extremely long context lengths.

the processing of individual prefill chunks is independent of the model output from the previous chunk.

Our key innovation lies in scheduling chunk  $i + 1$  immediately after chunk  $i$  completes the first pipeline stage (Figure 9b) during prefill. We call this approach sequence pipeline parallelism (SPP). This dense pipelining schedule efficiently parallelizes prefill processing, yielding near-linear speedup with increased GPU count, as described by:

$$T_p^{spp}(n, c) \simeq \frac{T_p(n, c)}{p_{spp}} + \frac{T_{comm}^{pp}(c)n}{c} \sim \frac{T_p(n, c)}{p_{spp}} \quad (8)$$

Here,  $T_p^{spp}(n, c)$  represents the SPP prefill time for  $n$  tokens with chunk size  $c$ ,  $T_p(n, c)$  is the standard prefill time,  $p_{spp}$  is the degree of sequence pipeline parallelism, and  $T_{comm}^{pp}(c)$  accounts for inter-stage communication time. The communication overhead term  $\frac{T_{comm}^{pp}(c)n}{c}$  becomes negligible for large  $n$ , leading to near-linear scaling.

This approach presents a distinctive advantage: the effectiveness of SPP remains independent of variations in input sequence length, unlike ring attention, where the degree of parallelism is closely tied to sequence length. Additionally, SPP supports batching and preemption, facilitating more efficient scheduling.

Our approach bears some resemblance to a technique proposed by Terapipe [27]. This work improves pipeline efficiency in model training. While both approaches leverage pipelining across sequence chunks, they differ significantly in their primary objectives and application contexts. TeraPipe aims to optimize throughput in the training phase by minimizing pipeline bubbles. In contrast, Mnemosyne applies a similar pipelining concept to the inference phase, specifically targeting latency reduction for online serving of long-context requests.

## 4.4 KV Parallelism

While SPP offers an effective mechanism to reduce prefill latency, it cannot be leveraged to optimize decode latency due to the cross-iteration dependency in auto-regressive decoding.

To address this challenge, we propose KV parallelism (KVP), a novel technique that effectively reduces decode latency by parallelizing KV-cache reads.

In KVP, the KV cache is sharded across multiple GPUs along the sequence dimension. During each iteration, we replicate the query token(s) across all GPUs and compute partial attention outputs based on the local KV-cache shard. These partial outputs are then combined using online-softmax [32]. A critical advantage of KVP over techniques like ring-attention and its derivatives is that the communication cost for KVP ( $T_{comm}^{kvp}$ ) is independent of the KV-cache length and only depends on the number of query tokens. This characteristic makes KVP extremely effective in managing decode latency for long-context requests.

The performance improvement of KVP can be modeled by the following equation:

$$T_d^{kvp}(n) \simeq \frac{T_d^{attn}(n)}{p_{kvp}} + (T_d(n) - T_d^{attn}(n)) + T_{comm}^{kvp} \quad (9)$$

Where  $T_d^{kvp}(n)$  is the decode time with KVP,  $T_d^{attn}(n)$  is the attention computation time,  $p_{kvp}$  is the degree of KV parallelism,  $T_d(n)$  is the total decode time, and  $T_{comm}^{kvp}$  is the communication overhead.

Our experiments reveal that KV parallelism is also effective in reducing the latency impact of prefills on the decodes of other batched requests in mixed batching scenarios. For instance, when processing a 4 million context length request, the P95 decode latency (for requests batched along) with even a small chunk of 128 tokens reaches almost 100ms.

The concept of KV parallelism extends naturally to chunked prefills. For long sequences, the communication cost of KV parallelism ( $T_{comm}^{kvp}(c)$ ) becomes significantly smaller than the attention computation itself. This relationship can be expressed as:

$$T_p^{kvp}(n, c) \simeq \frac{T_p^{attn}(n, c)}{p_{kvp}} + (T_p(n, c) - T_p^{attn}(n, c)) + T_{comm}^{kvp}(c) \quad (10)$$

Where  $T_p^{kvp}(n, c)$  is the prefill time for the  $i$ -th chunk with KVP,  $T_p^{attn}(n, c)$  is the attention computation time for the chunk,  $T_p(n, c)$  is the total prefill time for the chunk, and  $T_{comm}^{kvp}(c)$  is the communication overhead for the chunk.

To optimize resource utilization, we employ a dynamic growth strategy for KV parallel workers rather than pre-allocating all of them ahead of time. We define a maximum number of KV-cache tokens per request that would be managed by a single KV parallel worker. Initially, a single KV parallel worker is allocated to a request. Once we reach the limit of maximum KV tokens on a worker, we onboard a new KV parallel worker. This approach allows each KV parallel replica to independently batch other short requests while cooperatively processing the long request, ensuring efficient resource use across varied workloads.



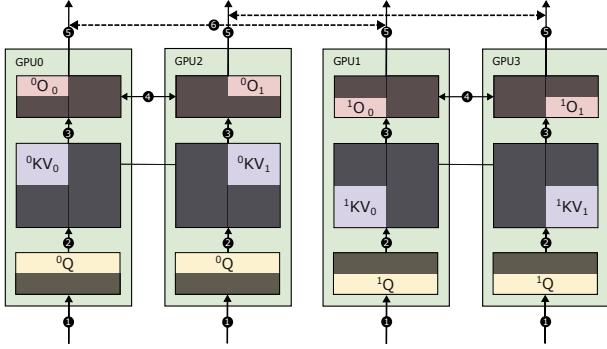


**Figure 11:** Combination of KV and Tensor Parallelism in Mnemosyne. This figure illustrates how KV Parallelism (horizontal distribution) and Tensor Parallelism (vertical distribution) work together to process long sequences efficiently. KV Parallelism splits the sequence across GPUs 0-1 and 2-3, while Tensor Parallelism divides computation within each KV shard across attention heads.

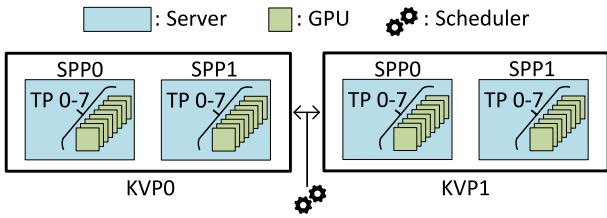
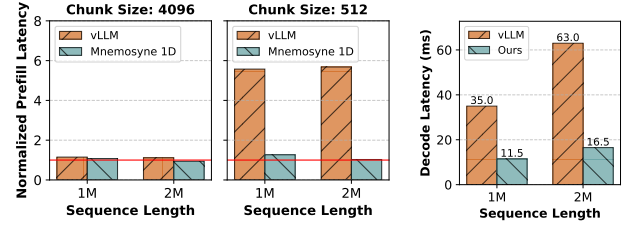


**Figure 12:** Mnemosyne’s 3D parallelism architecture: Combining Tensor Parallelism (TP), Sequence Pipeline Parallelism (SPP), and KV Parallelism (KVP) for scalable long-context LLM inference. Each KVP unit contains a full model replica with multiple pipeline stages, which in turn utilize tensor parallelism across GPUs within a server. This hierarchical design enables efficient processing of long sequences by accelerating both prefill and decode computing, while allowing flexible scheduling for mixed workloads.

#### 4.5 Mnemosyne 3D Parallelism

To meet the demanding requirements of both prefill and decode latency in long-context LLM inference, Mnemosyne introduces a novel 3D parallelism strategy. This approach combines sequence pipeline parallelism (SPP), KV parallelism (KVP), and tensor parallelism (TP) to effectively scale performance across hundreds of GPUs. The synergy of these parallelization techniques addresses different aspects of the inference process: SPP accelerates prefill computation, KVP reduces decode latency, and TP enhances both prefill and decode phases through model-level parallelization.

Determining the optimal configuration for this 3D parallelism is a complex task that requires careful consideration of multiple factors, including latency SLOs for both prefill and decode phases, the mix of request lengths in the workload, and the scaling efficiency of each parallelization dimension. Our experiments reveal that each parallelization technique has distinct scaling characteristics. SPP demonstrates excellent scalability, maintaining over 80% efficiency when scaled up



(a) Prefill latency normalized with respect to Striped Attention. (b) Decode latency.

**Figure 13:** Latency comparison: vLLM [3] vs Mnemosyne-1D TP for long context processing for Llama-3 8B with 8 H100 GPUs ( $p_{tp} = 8$ ). The  $3.8\times$  lower decode latency, and  $\sim 6\times$  lower prefill latency with small chunk size reflect the efficacy of various CPU optimizations implemented in Mnemosyne.

to 16 servers (Figure 15). This makes SPP particularly effective for reducing prefill latency in very long context scenarios. KVP, while crucial for meeting stringent decode latency targets, exhibits more limited scalability beyond 2-4 servers. This limitation stems from higher communication overhead compared to pipeline parallelism and parallelization limited to attention computation, which constrains its scaling efficacy due to Amdahl’s law.

Given the complexity of optimizing this 3D parallelism strategy, existing LLM inference simulators [6, 12] can be leveraged to identify optimal parallelization configuration based on the specific workload requirements.

## 5 Platform Optimizations

Efficient long-context LLM inference requires not only novel parallelization strategies but also careful platform-level optimizations. Mnemosyne extends the Sarathi-Serve framework [7] to address unique challenges that emerge at scale in three key areas: inter-process communication, model execution, and page-table management. As shown in Figure 13b, these optimizations yield up to  $4\times$  reduction in decode latency compared to existing systems. In rest of this section we detail our targeted engineering improvements in these areas, enabling Mnemosyne to handle multi-million token contexts effectively.

**Inter-process communication.** Traditional systems like vLLM and Sarathi-Serve [3, 7] rely on centralized schedulers to allocate memory and communicate page tables and sequence tokens to GPU workers in each iteration. This approach incurs significant overhead as sequence length increases. We mitigate this by replicating sequence state across the scheduler and all GPU workers, thereby reducing the communication volume. Additionally, we replace Ray [1] with ZeroMQ [4] for scheduler-worker communication, eliminating Global Interpreter Lock (GIL) [16] contention as we scale to hundreds of workers.

**Model execution.** We integrate Flashinfer [48] kernels, which efficiently distribute work across both query and KV tokens. This enhancement enables effective chunked prefill computation, crucial for processing extended contexts. To ensure strict latency targets even with small prefill chunks, we implement CUDA graphs for mixed batches.

**Page-table management.** We observe that copying large page tables from CPU to GPU memory in every iteration introduced considerable overhead. Our solution was to implement GPU-side page tables. We bootstrap the page table for a request upon initial on-boarding and subsequently transfer only delta updates to the GPU. This approach significantly reduces data movement between CPU and GPU memory and the latency impact of paged attention for long context lengths.

## 6 Evaluation

Mnemosyne’s parallelism strategies aim to enable efficient end-to-end inference for multi-million token contexts. We evaluate our system by addressing the following key questions:

- **Prefill Performance and Preemptibility** How does Mnemosyne improve prefill latency (TTFT) and preemptibility for long contexts compared to existing approaches? (§6.2)
- **Decode Performance** To what extent can Mnemosyne maintain low Time Between Tokens (TBT) as context length increases? (§6.3)
- **3D Parallelism Effectiveness** How does Mnemosyne’s 3D parallelism strategy balance the trade-offs between TTFT and TBT in end-to-end inference scenarios? (§6.4)
- **Throughput** What level of system throughput can Mnemosyne achieve while maintaining latency targets? (§6.5)
- **Adaptability** How well does Mnemosyne handle varying context lengths within a single deployment? (Addressed throughout §6.2-6.5)

Through answering these questions, we demonstrate Mnemosyne’s ability to meet the challenges of long-context LLM inference across a range of operating conditions.

### 6.1 Evaluation Setup

**Platform.** We implement Mnemosyne, with the additional optimizations and design innovations on top of the Sarathi-Serve framework [7] with the baseline optimizations described in Section 5. We implement the design changes for SPP, KVP, and 3D-Parallel strategies on this optimized baseline.

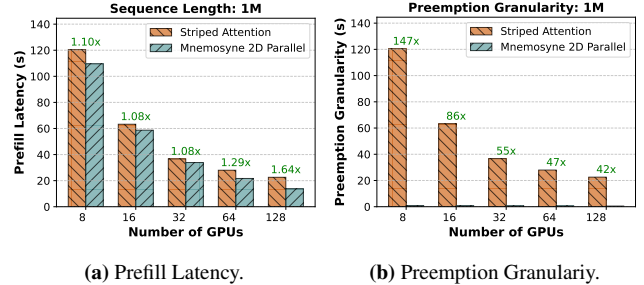


**Figure 14:** Performance comparison of Striped Attention vs. Mnemosyne 2D Parallel for 1M token sequences prefill with Llama-3 8B. Not only does Mnemosyne achieve better scaling efficiency for prefill computation, but also helps eliminate head of the line blocking by supporting fine-grained preemption.

**Models and datasets.** We use the models Llama-3 8B and Llama-3 70B with RoPE [43] scaling to support the context length of up to 10M tokens. Both, Llama-3 8B and Llama-3 70B have 8 KV heads allowing up to  $p_{tp} = 8$ .

Since Mnemosyne is an exact inference system, there is no approximation, or impact to the model accuracy from our design. The effect is solely limited to the latency and throughput of the system. Therefore, we do not depend on any scoring system or input datasets for our evaluation.

**Hardware.** We use up to 16 InfiniBand connected DGX-H100 systems [31]. Each DGX-H100 server has 8 NVIDIA H100 GPUs [34] with 80GB of high bandwidth memory each for a total of up to 128 GPUs. GPUs within a server are connected with NVLINK4.0 providing 900GBps bidirectional bandwidth. GPUs across different servers are connected with InfiniBand [37], offering 50GBps per GPU pair.

**System configurations.** We evaluate Mnemosyne with the following configurations:

- Mnemosyne 2D parallelism with SPP+TP, where  $p_{tp}$  is set to 8 (within the GPUs in a single server), and SPP is used to scale across servers for fast and pre-emptable prefill.
- Mnemosyne 2D parallelism with KVP+TP, where  $p_{tp} = 8$ , and KVP is used to scale across servers for fast decode.
- Mnemosyne 3D parallelism with KVP+SPP+TP, where  $p_{tp} = 8$ , and SPP and KVP are used to scale out the final Mnemosyne design.

### 6.2 Fast and Pre-emptable Prefill with SPP

As discussed in Section 4, SPP uses chunked prefills with efficient pipeline utilization to accelerate the prefill phase for long sequences.

**Baseline comparison.** The strongest baseline among previous work for long context prefill is Striped Attention [11]. Figure 14a compares the prefill latency of striped attention [11]

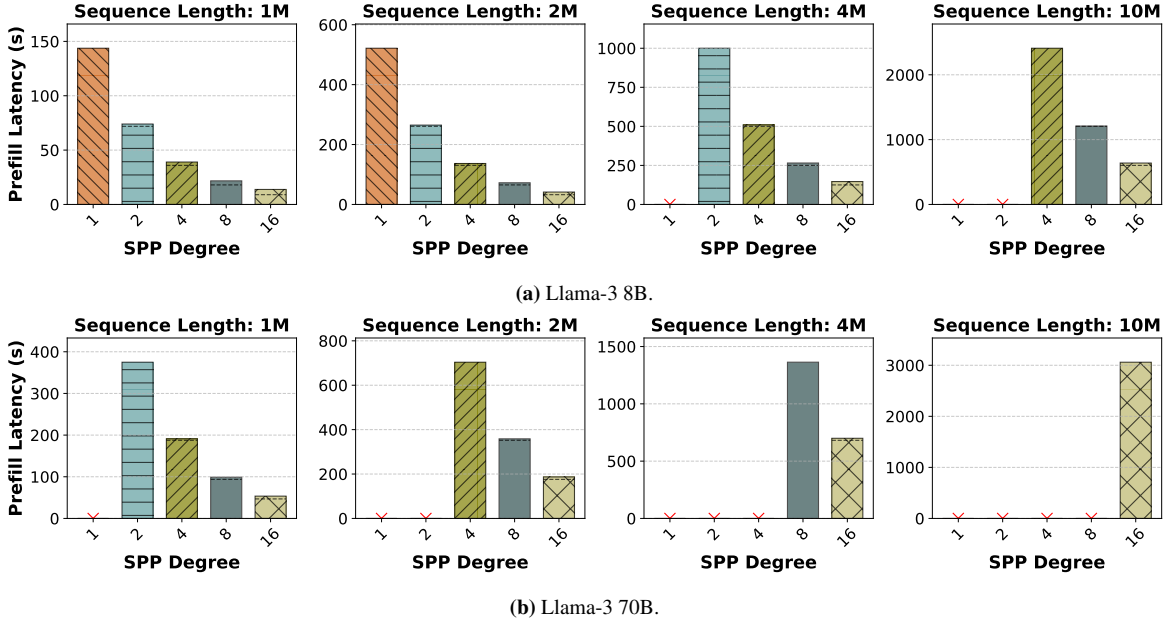


**Figure 15:** Scaling efficiency of Mnemosyne 2D Parallelism (SPP + TP) for Long Contexts prefill processing. Across both Llama-3 8B and 70B, Mnemosyne 2D exhibits near-linear (80%+ scaling efficiency) reductions in prefill latency as the SPP degree increases to operate with up to 128 H100 GPUs. Red crosses indicate infeasible configurations due to memory limitations.

with Mnemosyne 2D SPP+TP, for 1M tokens. We use a chunk size of 4K to show the TTFT latency without the effects from adaptive chunking due to mixed batching. This evaluation was run using 1 – 16 DGX-H100 servers. Mnemosyne 2D SPP+TP is 64% faster than striped attention using 128 GPUs (16 servers) when processing one million tokens, achieving TTFT latency under 15 seconds.

At the same time, Striped Attention can not support chunked prefills, leading to fully blocking long context prefills. This exacerbates the head-of-line blocking, as shown in Figure 14b, leading to delays as high as 120s with Striped attention, compared to just 62ms with Mnemosyne 2D SPP+TP. Mnemosyne 2D SPP+TP therefore achieves best of both world, with faster, and much more pre-emptable prefill phases than the strongest baseline.

**Scaling SPP to 10M.** Figure 15 shows the TTFT achieved by Mnemosyne 2D SPP+TP, as we increase the number of tokens from 1M to 10M, and vary the pipeline depth for SPP from 1 to 16 for Llama-3 8B and Llama-3 70B. The red crosses indicate configurations that are not feasible due to insufficient memory. Mnemosyne 2D SPP+TP achieves close to linear scaling efficiency with increasing pipeline depth, thanks to the optimizations described in Section 5.

We meet the 30 second TTFT for context length up to 2M on Llama-3 8B with 16 DGX servers. The strong scaling trendlines suggest that more DGX servers would enable even shorter TTFT latency for longer contexts.

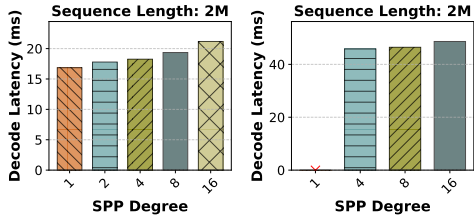
### 6.3 Fast Decode with KVP

Previous works do not support the decode phase for long context inference. Therefore, as a baseline, we show the decode phase performance (TBT) with Mnemosyne 2D SPP+TP. Note that the target SLO is 30ms.

**Baseline TBT with Mnemosyne 2D SPP+TP.** SPP is primarily a solution to unlock throughput and lower TTFT. Figure 16 shows the TBT achieved as SPP scales out for 2M context on Llama-3 8B and Llama-3 70B. Given the small overheads of pipeline parallelism, TBT gets worse with high SPP degree  $p_{spp}$ , with more visible effects on smaller models. This is because of the constant SPP communication overhead and higher computation time per pipeline stage going from Llama-3 8B to Llama-3 70B.

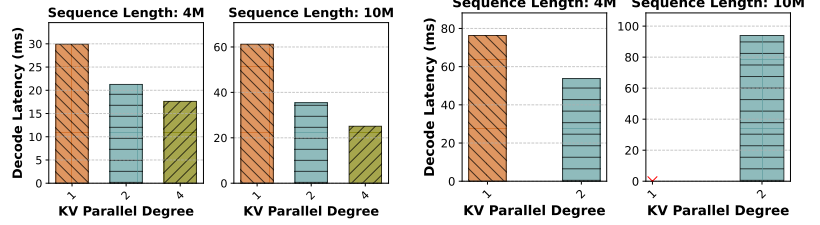
**Faster TBT with Mnemosyne 3D parallelism.** Figure 17 shows the TBT achieved for Llama-3 8B and Llama-3 70B with 4M and 10M context length in Mnemosyne 3D parallel KVP+SPP+TP setup, where  $p_{tp} = 8$ ,  $p_{spp} = 4$  for Llama-3 8B,  $p_{spp} = 8$  for Llama-3 70B, and  $p_{kvp}$  is varied.  $p_{spp} = 8$  was used for Llama-3 70B, since as shown in Figure 15b, longer context lengths for Llama-3 70B do not fit within  $p_{spp} = 4$ .

Figure 17 shows that increasing  $p_{kvp}$  brings down the TBT considerably, helping achieve interactivity targets. The latency benefit is not linear due to Amdahl’s law, but gets more pronounced with longer context length. Increasing  $p_{kvp}$  from 1 to 4, therefore using  $4\times$  the GPUs For Llama-3 8B, reduces TBT by only  $1.7\times$  for 4M context length, whereas for 10M context length this benefit increases to  $2.5\times$ . Since  $p_{kvp} = 1$  can meet



(a) Llama-3 8B (b) Llama-3 70B

**Figure 16:** Impact of SPP scaling on decode latency in Mnemosyne 2D Parallelism (SPP+TP,  $p_{tp} = 8$ ). Decode latency is only marginally affected even with pipeline consisting 16 stages.



(a) Llama-3 8B with  $p_{spp} = 4$ . (b) Llama-3 70B with  $p_{spp} = 8$ .

**Figure 17:** TBT Reduction with KV Parallelism in Mnemosyne 3D Parallelism in decode-only batches. For 10M context length decodes for Llama-3 8B,  $p_{kvp} = 2$  results in almost 40% reduction in latency, allows decode at the rate of  $\sim 30$  tokens per seconds.

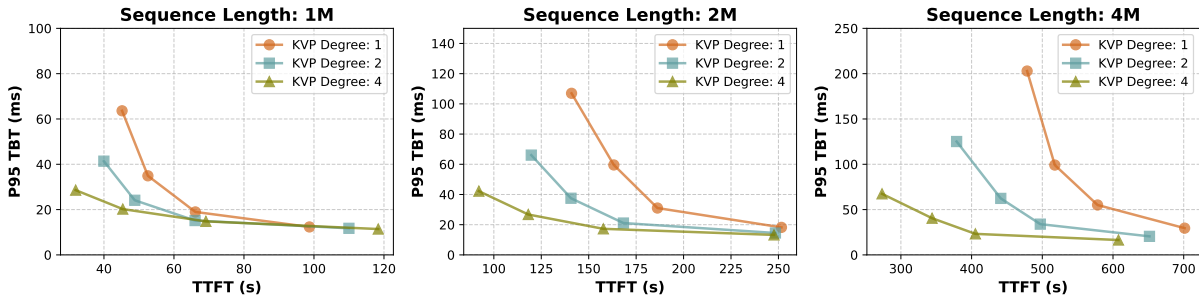


**Figure 18:** Trade-off Between TTFT and P95 TBT for Llama-3 8B using Mnemosyne 3D Parallelism ( $p_{tp} = 4$ ,  $p_{spp} = 4$ ) for varying KVP degrees and chunk sizes (32-256).

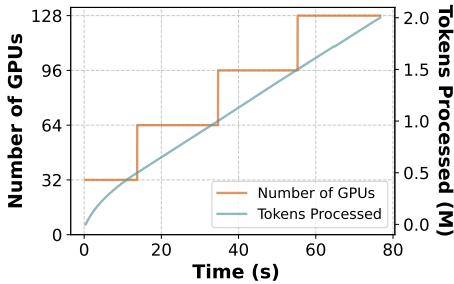


**Figure 19:** Number of GPUs needed over time when processing 2 million tokens with Llama-3 8B using Mnemosyne 3D with  $p_{tp} = 8$ ,  $p_{kvp} = 4$ , and  $p_{spp} = 4$ . Mnemosyne starts with a single KVP worker group participating (4 servers) and progressively onboards 12 more servers as sequence length increases. By dynamically growing resource allocation, Mnemosyne maintains near consistent per iteration latency.

TBT target SLOs until 4M context for Llama-3 8B, and until 2M context for Llama-3 70B, we propose KVP scaling only if the input context is beyond those respective lengths.

## 6.4 End-to-end inference with Mnemosyne 3D

Finally, we evaluate Mnemosyne 3D parallelism with mixed batching of prefills and decodes. The main contribution of this

work is to be able to serve multi-million context lengths end-to-end, while meeting the TTFT and TBT SLOs of interactive jobs. This requires mixed batching per iteration. We evaluate the trade-off between TTFT and TBT with our design.

**TTFT vs TBT trade-off.** We sweep the space of various chunk sizes for the chunked prefill, and also vary  $p_{kvp}$ , while keeping  $p_{spp} = 4$ . Figure 18 shows the results on Llama-3 8B. For a given  $p_{kvp}$ , increasing the chunk size, reduces TTFT (prefill latency), since it requires fewer iterations. At the same time, it increases TBT, since each batched iteration takes longer to execute. Therefore, for sequence length 1M with  $p_{kvp} = 1$ , the green line shows the left-most triangle at largest chunk size, and the right-most triangle at the smallest chunk size. For a given chunk size, increasing  $p_{kvp}$  helps reduce both TTFT and TBT in most cases, thus helping reach more optimal points in this trade-off space. Indeed, lower  $p_{kvp}$  achieves better TTFT latency in cases with lower arithmetic intensity (due to small chunk size), as exemplified by the right-most points for 1M context length. As we increase the arithmetic intensity (e.g., 2M context length), we see increasing  $p_{kvp}$  achieving the same performance for the smallest chunk size, and, finally, decreasing TTFT for 4M context length.

The main takeaway from Figure 18 is the combination of the proposed Mnemosyne parallelization strategies creates more choices in the TBT/TTFT trade-off space, which is significant when operating under tight latency SLO spec-



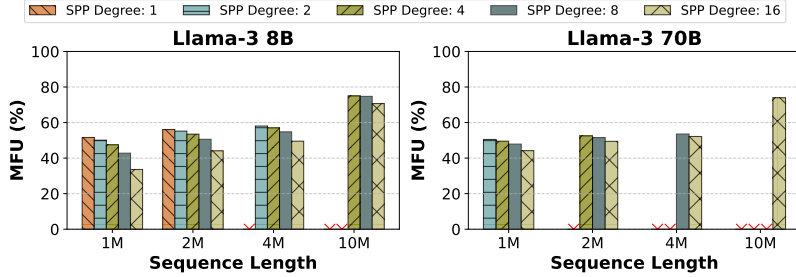


**Figure 20:** Model FLOPS Utilization [13] (MFU) for Mnemosyne 2D Parallelism (TP + SPP). The system consistently achieves 50-60% utilization across different sequence lengths and parallelism degrees.

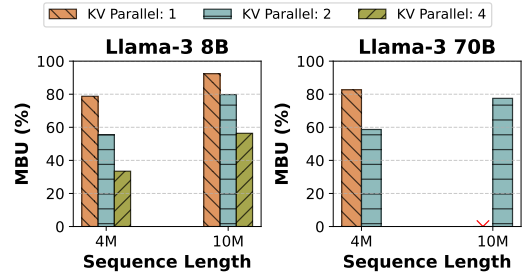


**Figure 21:** Model Bandwidth Utilization (MBU) for Mnemosyne 2D Parallelism (TP + KVP).

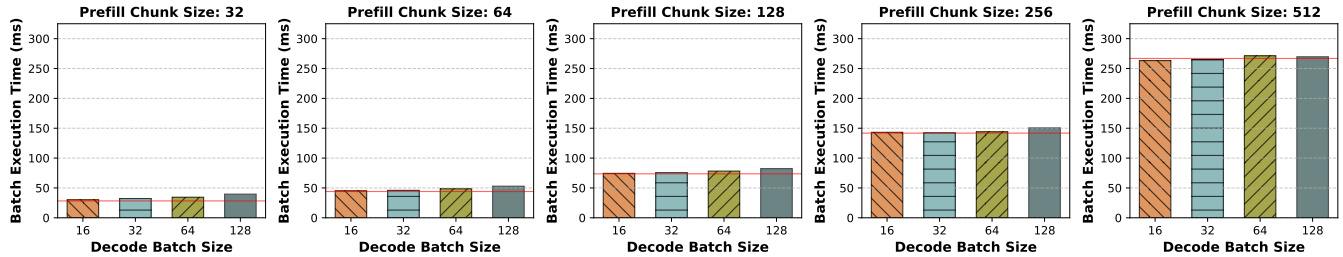


**Figure 22:** P95 mixed batch execution latency with chunked prefill of a long request (1M) and several decode requests (1K each) for Llama-3 8B on 8 H100s (TP). Results are shown comparing the batch execution time as we vary the chunk size for the prefill, and the number of decode phases batched. Red line represents the execution time of the batch with the chunked prefill running alone without any decode phases batched.

ifications. A system with a more sparsely populated set of configuration options could render the same TBT/TTFT SLO pair infeasible. In contrast, Mnemosyne increases the feasibility range over a broader set of configuration options in this trade-off space.

**Timeline of KVP instance addition.** Figure 19 shows the timeline for Mnemosyne 3D processing 2 million tokens using Llama-3 70B for one of the runs in Figure 18 with  $p_{tp} = 8$ ,  $p_{kvp} = 4$ , and  $p_{spp} = 4$ . Mnemosyne 3D starts with  $p_{kvp} = 1$ ,  $p_{tp} = 8$ , and  $p_{spp} = 4$ , using 32 GPUs. Then, a KVP instance of 32 more GPUs is added, one at a time based on the sequence length processed so far, until it reaches the max of 128 GPUs. Increasing context length and increasing parallelism act as opposing forces allowing consistent iteration execution time.

## 6.5 Enabling high throughput

The final goal for Mnemosyne to achieve is high throughput. We evaluate the throughput of Mnemosyne 3D system in two ways: first, Model Flops Utilization (MFU) and Model Bandwidth Utilization (MBU) to show that the hardware resources are well utilized, and second, Impact of batching requests on latency (minimal impact enables high throughput).

**MFU and MBU.** MFU and MBU are metrics to measure the hardware utilization for compute-bound phases and memory-bound phases respectively. These metrics were coined re-

cently and have since been widely used to report the efficiency of LLM inference and training systems [2, 13]. In LLM inference, prefill phases are compute-bound, and decode phases are memory-bound [35, 36]. Therefore, in Figures 20 and 21, we show the MFU and MBU in prefill phase of Mnemosyne 2D SPP+TP, and decode phase of Mnemosyne 2D KVP+TP, respectively. We achieve between 50-75% MFU, which is very high, even when compared to training-optimized systems [13]. For MBU, we reach as high as 92% representing very efficient use of memory bandwidth. As we increase the degrees of parallelism to achieve lower latency, the utilization decreases, as expected.

**Batching efficiency.** Figure 22 shows the impact of batching multiple decode phases together with chunked prefill phases. The main takeaway is that increasing batch size up to 128 requests does not increase the batch execution time more than 5%. This enables large batch sizes and high throughput. Furthermore, the figure also underscores the impact of increasing chunk size on the TBT, or, the batch execution time.

## 7 Designing Systems with Mnemosyne

Section 6 shows that Mnemosyne enables a system to serve varying context lengths as long as 10M length, with low latency and high throughput. Designing with Mnemosyne needs a few more steps.

**Scheduling policy.** Mnemosyne enables preemption of prefill phases, and adaptive chunking to trade-off TTFT and TBT, both of which require a dynamic scheduling policy. Additionally, it opens up another rich space for scheduling policies to help increase the system throughput - independent scheduling of KVP instances. Since each KVP instance has a full model replica within it, unless the instances are working together on a long context inference, they can be scheduled separately for shorter requests. This presents a huge opportunity for throughput optimization.

**Finding the right parallelism.** The 3D parallelism introduced by Mnemosyne provides a rich space for trading off TTFT, TBT, and throughput. This calls for profiling stage with representative traces to find the right parallelism fit.

**Online vs offline inference.** Despite strong scaling of SPP and KVP parallelism meeting interactive latency targets for TTFT (e.g., 30 seconds for 10M context length) would require prohibitive number of GPUs. We envision that longer context lengths will either need approximation, or a disaggregated setup with prefill and decode phases separated as proposed in previous works [35, 51]. A disaggregated setup allows offline context building with slower prefill phase, which is then sent over to a decode-optimized system to meet the interactive TBT latency SLOs.

**Exact vs approximate.** Even though in this paper, we present Mnemosyne as a solution without any approximation to serve long context, it does not preclude the parallelism strategies to be used with approximate techniques described in Section 8.

## 8 Related Work

**LLMs for long context.** Recent research has focused on effectively training and efficiently serving long-context LLM models. Some propose new attention parallelism techniques as more efficient solutions to enable long context [11, 26, 30]. We discuss and compare them in detail in Sections 3.2 and 6. Concurrently, compute kernel optimizations [14, 20, 48] have enhanced parallelism across different dimensions within a GPU, enabling efficient computation long contexts. In addition, techniques like LongRoPE [15] identify effective rescale factors and adapt progressive extension strategy, allowing re-scaling positional embeddings and extending context window beyond million tokens for existing LLMs without the need for additional fine-tuning. A similar idea to SPP without adaptive chunking, called token-parallelism, was used in TeraPipe [27] to parallelize the different micro-batches of a mini-batch along the token dimension in order to reduce pipeline bubbles and improve throughput during training. In Mnemosyne, we create small mixed-batches of chunked prefill and decodes and then parallelize these mixed batches to maintain latency targets during inference.

**Approximate alternatives.** To reduce computational complexity and enhance serving efficiency, State Space Mod-

els (SSMs) [17, 18] propose alternatives to the traditional attention-based architecture. Other approaches, such as locality-sensitive hashing [24], compressive attention [33], and prompt or KV cache compression [23, 25, 50], aim to reduce both the computational and memory footprint of transformer-based LLMs. While these approaches trade accuracy for reduced computation and memory needs—potentially enabling long-context inference – we focus on transformer-based models that maintain accuracy by retaining the full context.

**LLM inference efficiency.** To improve LLM inference serving efficiency, researchers have proposed various techniques including chunked prefills [8], prefill-decode disaggregation [35, 51], elastic parallelism [47], and distributed KV cache [28]. Inference requests at million-token scale introduce a new set of challenges (Section 3) and require careful designs to incorporate these methods effectively at scale. In a concurrent work, Mooncake [38], chunked pipeline parallelism was proposed that is similar to SPP for long context inference serving but focusing solely on prefill requests with up to 128K tokens. While some other mechanisms (i.e., offloading [25, 41]) address memory bottlenecks, compute remains the primary bottleneck for online long context inference serving (Section 2.1). Nonetheless, these techniques can be useful for offline processing in resource constrained situations.

## 9 Conclusion

Long context LLM inference use-cases continue to grow, constantly pushing the boundary of what constitutes as "long" context. With Mnemosyne, we propose a set of novel parallelism strategies that enable serving end-to-end inference for context lengths scaling at least up to 10M tokens, with fast prefill and decode phases, meeting the interactive latency target of TTFT up to 2M tokens, and that of TBT up to 10M tokens. Furthermore, Mnemosyne enables variable context requests on input, and mixed batching with adaptive chunking. This allows dynamic scheduling based on deadlines, enabling higher system throughput with latency guarantees while supporting input of varying context lengths.

## References

- [1] Apache Ray. <https://docs.ray.io/en/latest/index.html>.
- [2] LLM Inference Performance Engineering: Best Practices. <https://www.databricks.com/blog/llm-inference-performance-engineering-best-practices>.
- [3] vLLM: Easy, fast, and cheap LLM serving for everyone. <https://github.com/vllm-project/vllm>.

- [4] ZeroMQ. <https://zeromq.org/>.
- [5] Amey Agrawal, Anmol Agarwal, Nitin Kedia, Jayashree Mohan, Souvik Kundu, Nipun Kwatra, Ramachandran Ramjee, and Alexey Tumanov. Etalon: Holistic Performance Evaluation Framework for LLM Inference Systems, 2024.
- [6] Amey Agrawal, Nitin Kedia, Jayashree Mohan, Ashish Panwar, Nipun Kwatra, Bhargav S Gulavani, Ramachandran Ramjee, and Alexey Tumanov. Vidur: A Large-Scale Simulation Framework For LLM Inference. *ML-Sys*, 2024.
- [7] Amey Agrawal, Nitin Kedia, Ashish Panwar, Jayashree Mohan, Nipun Kwatra, Bhargav S Gulavani, Alexey Tumanov, and Ramachandran Ramjee. Taming Throughput-Latency Tradeoff in LLM Inference with Sarathi-Serve. *OSDI*, 2024.
- [8] Amey Agrawal, Ashish Panwar, Jayashree Mohan, Nipun Kwatra, Bhargav S. Gulavani, and Ramachandran Ramjee. SARATHI: Efficient LLM Inference by Piggybacking Decodes with Chunked Prefills, 2023.
- [9] Joshua Ainslie, James Lee-Thorp, Michiel de Jong, Yury Zemlyanskiy, Federico Lebrón, and Sumit Sanghai. GQA: Training Generalized Multi-Query Transformer Models from Multi-Head Checkpoints, 2023.
- [10] Sparsh Bhasin. Enhancing LLM Context Length with RoPE Scaling. <https://blog.monsterapi.ai/blogs/enhancing-llm-context-length-with-rope-scaling>, 2024.
- [11] William Brandon, Aniruddha Nrusimha, Kevin Qian, Zachary Anknor, Tian Jin, Zhiye Song, and Jonathan Ragan-Kelley. Striped attention: Faster ring attention for causal transformers. *arXiv preprint arXiv:2311.09431*, 2023.
- [12] Jaehong Cho, Minsu Kim, Hyunmin Choi, Guseul Heo, and Jongse Park. Llmservingsim: A hw/sw co-simulation infrastructure for llm inference serving at scale, 2024.
- [13] Aakanksha Chowdhery, Sharan Narang, Jacob Devlin, Maarten Bosma, Gaurav Mishra, Adam Roberts, Paul Barham, Hyung Won Chung, Charles Sutton, Sebastian Gehrmann, et al. PaLM: Scaling Language Modeling with Pathways. *Journal of Machine Learning Research*, 24(240):1–113, 2023.
- [14] Tri Dao. FlashAttention-2: Faster Attention with Better Parallelism and Work Partitioning, 2023.
- [15] Yiran Ding, Li Lyna Zhang, Chengruidong Zhang, Yuanyuan Xu, Ning Shang, Jiahang Xu, Fan Yang, and Mao Yang. Longrope: Extending llm context window beyond 2 million tokens. *arXiv preprint arXiv:2402.13753*, 2024.
- [16] Roger Eggen and Maurice Eggen. Thread and process efficiency in Python. In *PDPTA*, 2019.
- [17] Albert Gu and Tri Dao. Mamba: Linear-time sequence modeling with selective state spaces. *arXiv preprint arXiv:2312.00752*, 2023.
- [18] Albert Gu, Karan Goel, and Christopher Ré. Efficiently modeling long sequences with structured state spaces. *arXiv preprint arXiv:2111.00396*, 2021.
- [19] Connor Holmes, Masahiro Tanaka, Michael Wyatt, Ammar Ahmad Awan, Jeff Rasley, Samyam Rajbhandari, Reza Yazdani Aminabadi, Heyang Qin, Arash Bakhtiari, Lev Kurilenko, and Yuxiong He. DeepSpeed-FastGen: High-throughput Text Generation for LLMs via MII and DeepSpeed-Inference, 2024.
- [20] Ke Hong, Guohao Dai, Jiaming Xu, Qiuli Mao, Xiuhong Li, Jun Liu, Kangdi Chen, Yuhan Dong, and Yu Wang. FlashDecoding++: Faster Large Language Model Inference on GPUs. *arXiv preprint arXiv:2311.01282*, 2023.
- [21] Yanping Huang, Youlong Cheng, Ankur Bapna, Orhan Firat, Dehao Chen, Mia Chen, HyoukJoong Lee, Jiquan Ngiam, Quoc V Le, Yonghui Wu, et al. Gpipe: Efficient training of giant neural networks using pipeline parallelism. *Advances in neural information processing systems*, 32, 2019.
- [22] Jacob Jackson. Announcing Supermaven 1.0. <https://supermaven.com/blog/announcing-supermaven-1.0>.
- [23] Huiqiang Jiang, Qianhui Wu, Xufang Luo, Dongsheng Li, Chin-Yew Lin, Yuqing Yang, and Lili Qiu. Longllm-lingua: Accelerating and enhancing llms in long context scenarios via prompt compression. *arXiv preprint arXiv:2310.06839*, 2023.
- [24] Nikita Kitaev, Łukasz Kaiser, and Anselm Levskaya. Reformer: The efficient transformer. *arXiv preprint arXiv:2001.04451*, 2020.
- [25] Wonbeom Lee, Jungi Lee, Junghwan Seo, and Jaewoong Sim. {InfiniGen}: Efficient generative inference of large language models with dynamic {KV} cache management. In *18th USENIX Symposium on Operating Systems Design and Implementation (OSDI 24)*, pages 155–172, 2024.

- [26] Shenggui Li, Fuzhao Xue, Chaitanya Baranwal, Yongbin Li, and Yang You. Sequence parallelism: Long sequence training from system perspective. *arXiv preprint arXiv:2105.13120*, 2021.
- [27] Zhuohan Li, Siyuan Zhuang, Shiyuan Guo, Danyang Zhuo, Hao Zhang, Dawn Song, and Ion Stoica. TeraPipe: Token-Level Pipeline Parallelism for Training Large-Scale Language Models. *arXiv preprint arXiv:2102.07988*, 2021.
- [28] Bin Lin, Chen Zhang, Tao Peng, Hanyu Zhao, Wencong Xiao, Minmin Sun, Anmin Liu, Zhipeng Zhang, Lanbo Li, Xiafei Qiu, Shen Li, Zhigang Ji, Tao Xie, Yong Li, and Wei Lin. Infinite-llm: Efficient llm service for long context with distattention and distributed kvcache, 2024.
- [29] Hao Liu, Wilson Yan, Matei Zaharia, and Pieter Abbeel. World Model on Million-Length Video And Language With Blockwise RingAttention, 2024.
- [30] Hao Liu, Matei Zaharia, and Pieter Abbeel. Ring Attention with Blockwise Transformers for Near-Infinite Context, 2023.
- [31] Microsoft Azure. ND-H100-v5 sizes series. <https://learn.microsoft.com/en-us/azure/virtual-machines/sizes/gpu-accelerated/ndh100v5-series?tabs=sizenetwork>, 2024.
- [32] Maxim Milakov and Natalia Gimelshein. Online normalizer calculation for softmax. *arXiv preprint arXiv:1805.02867*, 2018.
- [33] Tsendsuren Munkhdalai, Manaal Faruqui, and Siddharth Gopal. Leave no context behind: Efficient infinite context transformers with infini-attention. *arXiv preprint arXiv:2404.07143*, 2024.
- [34] NVIDIA. DGX H100: AI for Enterprise. <https://www.nvidia.com/en-us/data-center/dgx-h100/>, 2024.
- [35] Pratyush Patel, Esha Choukse, Chaojie Zhang, Íñigo Goiri, Aashaka Shah, Saeed Maleki, and Ricardo Bianchini. Splitwise: Efficient generative LLM inference using phase splitting. In *ISCA*, 2024.
- [36] Pratyush Patel, Esha Choukse, Chaojie Zhang, Íñigo Goiri, Brijesh Warriar, Nithish Mahalingam, and Ricardo Bianchini. Polca: Power oversubscription in llm cloud providers, 2023.
- [37] Gregory F Pfister. An introduction to the InfiniBand architecture. *High performance mass storage and parallel I/O*, 42(617-632):10, 2001.
- [38] Ruoyu Qin, Zheming Li, Weiran He, Mingxing Zhang, Yongwei Wu, and Xinran Xu Weimin Zheng. Mooncake: A KVCache-centric Disaggregated Architecture for LLM Serving, 2024.
- [39] M Reid, N Savinov, D Teplyashin, Lepikhin Dmitry, T Lillicrap, JB Alayrac, R Soricut, A Lazaridou, O Firat, et al. Gemini 1.5: Unlocking multimodal understanding across millions of tokens of context. *arXiv preprint arXiv:2403.05530*, 2024.
- [40] Ying Sheng, Shiyi Cao, Dacheng Li, Banghua Zhu, Zhuohan Li, Danyang Zhuo, Joseph E Gonzalez, and Ion Stoica. Fairness in Serving Large Language Models. *arXiv preprint arXiv:2401.00588*, 2023.
- [41] Ying Sheng, Lianmin Zheng, Binhang Yuan, Zhuohan Li, Max Ryabinin, Daniel Y. Fu, Zhiqiang Xie, Beidi Chen, Clark Barrett, Joseph E. Gonzalez, Percy Liang, Christopher Ré, Ion Stoica, and Ce Zhang. Flexgen: High-throughput generative inference of large language models with a single gpu, 2023.
- [42] Mohammad Shoeybi, Mostofa Patwary, Raul Puri, Patrick LeGresley, Jared Casper, and Bryan Catanzaro. Megatron-lm: Training multi-billion parameter language models using gpu model parallelism. *arXiv preprint arXiv:1909.08053*, 2019.
- [43] Jianlin Su, Murtadha Ahmed, Yu Lu, Shengfeng Pan, Wen Bo, and Yunfeng Liu. Roformer: Enhanced transformer with rotary position embedding. *Neurocomputing*, 568, 2024.
- [44] Claude team. Prompt Caching (beta). <https://docs.anthropic.com/en/docs/build-with-claude/prompt-caching>.
- [45] Gemini team. Context caching. <https://ai.google.dev/gemini-api/docs/caching>.
- [46] Gradient team. Scaling Rotational Embeddings for Long-Context Language Models. <https://gradient.ai/blog/scaling-rotational-embeddings-for-long-context-language-models>.
- [47] Bingyang Wu, Shengyu Liu, Yinmin Zhong, Peng Sun, Xuanzhe Liu, and Xin Jin. Loongserve: Efficiently serving long-context large language models with elastic sequence parallelism. *arXiv preprint arXiv:2404.09526*, 2024.
- [48] Zihao Ye, Lequn Chen, Ruihang Lai, Yilong Zhao, Size Zheng, Junru Shao, Bohan Hou, Hongyi Jin, Yifei Zuo, Liangsheng Yin, Tianqi Chen, and Luis Ceze. Accelerating Self-Attentions for LLM Serving with FlashInfer, February 2024.



- [49] Gyeong-In Yu, Joo Seong Jeong, Geon-Woo Kim, Soojeong Kim, and Byung-Gon Chun. Orca: A Distributed Serving System for Transformer-Based Generative Models. In *OSDI*, 2022.
- [50] Zhenyu Zhang, Ying Sheng, Tianyi Zhou, Tianlong Chen, Lianmin Zheng, Ruisi Cai, Zhao Song, Yuandong Tian, Christopher Re, Clark Barrett, Zhangyang Wang, and Beidi Chen.  $\$H_{20}\$$ : Heavy-Hitter Oracle for Efficient Generative Inference of Large Language Models. In *Conference on Parsimony and Learning (Recent Spotlight Track)*, 2023.
- [51] Yinmin Zhong, Shengyu Liu, Junda Chen, Jianbo Hu, Yibo Zhu, Xuanzhe Liu, Xin Jin, and Hao Zhang. DistServe: Disaggregating Prefill and Decoding for Goodput-optimized Large Language Model Serving, 2024.